Chemical Papers (2021) 75:3061–3072
https://doi.org/10.1007/s11696-021-01546-6

ORIGINAL PAPER

Antibody-oriented immobilization for newcastle disease virus detection using label free electrochemical immunosensor

Parviz Norouzi[1,2] · Mohammad Nezamoddini[1] · Mohammad Reza Safarnejad[3]

Received: 6 October 2020 / Accepted: 28 January 2021 / Published online: 16 February 2021

Abstract

In this work, a new label free electrochemical immunosensor was designed to detect Newcastle disease virus (NDV). The immunosensor was constructed by modification of a glassy carbon electrode surface with multi wall carbon nanotubes, gold nanoparticles (AuNPs), 11-Mercapto Undecanoic acid (MUA) and 3-Mercapto Propionic acid. Then, it was stabilized by self-assembly and protein G (PrG) immobilized using 1-ethyl3-(3-dimethylaminopropyl) carbodiimide (EDC) and N-Hydroxy Succinimide to oriented fixation of the antibody. The quantitative measurement of NDV was evaluated by square wave voltammetry method. The determination step was based on the formation of immunocomplex between the antigen and oriented antibody, which caused current decreased in $[Fe(CN)_6]/K_4[Fe(CN)_6]$ redox reaction. The response value was directly proportional to the concentrations of NDV. Scanning electron microscope, XRD, UV and FTIR methods were used to characterize the electrode surface. Also, the electrochemical electrode surface behavior at each step of modification was evaluated by cyclic voltammetry and electrochemical impedance spectroscopy methods. The parameters affecting the performance of the immunosensor such as amount of MWCNT, electrodeposition time of AuNPs, concentration and loading time of PrG, the antibody concentration and antigen incubation time were optimized. The biosensor showed detection limit of 1.6 $EID_{50}ml^{-1}$ and linear range of 10 to 10^5 $EID_{50}ml^{-1}$. The proposed immunosensor showed adequate reproducibility (RSD 6%) and stability (up to one month), which showed that it could be used as a sensitive device for agriculture applications.

Keywords Newcastle disease virus · Label free electrochemical immunosensors · Antibody-oriented immobilization · Protein G

Introduction

Newcastle disease virus (NDV) is one of the most important herd-breeding birds diseases, which was first diagnosed in Newcastle's, England, in 1926. The disease, which is contagious and fatal, has a viral agent and affects many chickens if not vaccinated (Li et al. 2019). NDV is a single-stranded negative-sense RNA virus, which belongs to the genus Rubulavirus of the family Paramyxoviridae. Considering high prevalence of the disease and the rapid spread of poultry and other bird species, it is a serious threat to the poultry industry worldwide (Dhar et al. 2018; Wang et al. 2019). For this reason, many efforts have been made for its detection at the golden time.

So far, various qualitative and quantitative techniques such as different types of polymerase chain reaction (PCR) (Chen et al. 2008, 2018; Cong et al. 2018; Fellahi et al. 2016; Laamiri et al. 2018; Mirzaei et al. 2018, 2020; Sutton et al. 2019; Wang et al. 2017; Yao et al. 2019; Zhang et al. 2020, 2019), hemagglutination inhibition (HI) (Chaka et al. 2015), agar Gel precipitation (De Wit et al. 1992), Latex agglutination tests (Thirumurugan et al. 1997), enzyme-linked immunosorbent assay (ELISA) (Garnier et al. 2017; Zhang et al. 2017), immunofluorescence test (Kothlow et al. 2008) and immunochromatographic strip (Li et al. 2019) have been employed to determine NDV. Although these techniques have been widely used for the determination of NDV in infected samples

✉ Parviz Norouzi
norouzi@khayam.ut.ac.ir

[1] Center of Excellence in Electrochemistry, University of Tehran, Tehran, Iran

[2] Endocrinology and Metabolism Research Center, Tehran University of Medical Sciences, Tehran, Iran

[3] Agricultural Research Education and Extension Organization (AREEO), Iranian Research Institute of Plant Protection, Tehran, Iran

and even some of them are highly sensitive (such as RT-PCR), but they are costly and severely time consuming and also require advanced equipment and professional technicians (Thinh et al. 2018). Therefore, electrochemical immunosensors have been considered for such detection applications due to their high measuring speed, simplicity and sensitivity.

In recent years, electrochemical immunosensors have been used to detect antigens for clinical purposes (Ghanavati et al. 2020; Mollarasouli et al. 2018; Wang et al. 2018), environmental monitoring (Fan et al. 2012; González-MartÍnez et al. 1998) and food industry (Alves et al. 2017; Taghdisi et al. 2018). These immunosensors are simple, fast, highly sensitive, accurate, portable and economical (Hosu et al. 2017). The electrochemical immunosensors could be divided into labeled (Huang et al. 2020) and label free groups (Wei et al. 2020), where the antibodies bind to the surface of the transducer as recognition element and interact directly with their respective antigen and produces electrochemical signal. Label free electrochemical immunosensors compared with the labeled types have simpler design and do not require secondary antibody and complex labeling steps as well (Ebrahimi et al. 2019; Haji-Hashemi et al. 2017, 2018, 2019).

Thinh et al. for the first time in 2019 used a label free electrochemical immunosensor to detect NDV. In which, they stabilized the chicken egg yolk antibodies (IgY) with a random orientation on a layer of alkane thiols that self-assembled on their gold surface to detect NDV (Garnier et al. 2017). In the design of electrochemical immunosensors the layers configuration at the electrode surface is very important, because it could strongly affect the performance of the immunosensor (Thinh et al. 2018). As a consequence, the modification of the electrode surface with nanomaterials has drawn intense attention since it can help to improve the surface properties of the electrode toward the analyte detection. Among them, MWCNTs (Eissa et al. 2018b; Martínez Rojas 2020) and AuNPs (Tang et al. 2018; Xiao et al. 2020) are the most widely used nanomaterials, due to their excellent properties such as ease of preparation, excellent electrical properties, good biocompatibility and large surface-to-mass ratio (Paiva et al. 2017). Furthermore, gold surface decoration using self-assembled monolayers for bioaccumulation is one of the most applicable and popular strategies on this approach. In this method, molecules such as alkane thiols, which have sulfur terminals, can spontaneously be accumulated on the gold electrode surface. On the other side of these molecules, functional groups could be placed, which could be activated and being used for covalent binding to proteins (Mackiewicz et al. 2018). In the case of carboxylic acid, the activation is usually performed through single step using 1-ethyl3-(3-dimethylaminopropyl) carbodiimide (EDC) and N-Hydroxy Succinimide(NHS) (Eissa et al. 2018a).

Also, one of the most important steps in the design of electrochemical immunosensors is the antibody stabilization on the surface of electrode. Although, the antibodies could be readily stabilized by various procedures such as physical adsorption (Haji-Hashemi et al. 2018) or covalent bonding of amino groups to modified electrode surfaces (Afkhami et al. 2017), the efficiency of immunocomplex formation by these methods is low, which could be due to the random orientation of antibodies, denaturation and sterile hindrance. For this purpose, antibody binding proteins, such as protein G (PrG) could be used. This protein can bind specifically to the non-antigenic region of many mammalian immunoglobulins and make antigen binding sites well accessible and with minimal sterile hindrance (Berto et al. 2019). It has been found that oriented and appropriate antibody immobilization on the surface immunosensor could increase the binding capacity of the antigen by approximately 2 to 8 times compared to random immobilization, which could increase sensitivity, linearity and reduce the detection limit (Lin et al. 2019). Random orientation of the antibodies are known to be responsible for having less binding capacities, thus having the appropriate antibody immobilization method would be essential for immunosensors design and fabrication. About the oriented type of antibodies immobilization, the main advantage is that the active binding sites would be more effectively accessible. Moreover, using disulfide bridges for having oriented immobilization is simple, quick and cost-effective (Baniukevic et al. 2013; Kausaite-Minkstimiene et al. 2010; Makaraviciute et al. 2014).

In this work, antibody-oriented stabilization was chosen by PrG to detect NDV. To reach this goal, the glassy carbon electrode (GCE) surface was first coated with MWCNT and t with AuNPs simultaneously. Then, by adding 11-Mercapto Undecanoic acid (MUA) and 3-Mercapto Propionic acid (MPA) self-assembled monolayers was formed on the surface. Subsequently, PrG was linked to MUA and MPA carboxyl groups, which were previously activated by the EDC and NHS. Finally, the anti-NDV antibody, as the bioreceptor with the appropriate orientation was stabilized on the PrG, so its antigenic sites were accessible for further interactions. For characterization of the modified electrode surface, scanning electron microscope (SEM), XRD, UV and FTIR methods were used. In addition, the fabrication process of the immunosensor was characterized with cyclic voltammetry (CV) and electrochemical impedance spectroscopy (EIS).

Experimental

Materials

NDV B1 virus protein (NDV-B1), NDV LaSota virus protein (10^6 $EID_{50}ml^{-1}$ (50 percent Embryo Infectious Dose))

and anti-NDV (1 $mgml^{-1}$) against it were obtained from Razi Vaccine and Serum Research Institute, Karaj, Iran. All chemicals; protein G (PrG), bovine serum albumin (BSA), Gold (III) chloride hydrate ($HAuCl_4{\cdot}4H_2O$, 99%), 3-Mercapto Propionic acid (MPA) 99%, 11-Mercapto Undecanoic acid (MUA) 95%, 1-ethyl3-(3-dimethylaminopropyl) carbodiimide–HCL (EDC), N-Hydroxy Succinimide (NHS) 98%, potassium ferricyanide ($K_3Fe(CN)_6$), potassium ferrocyanide ($K_4Fe(CN)_6$) and potassium chloride (KCl) were purchased from Sigma-Aldrich, and used without further purification. Multiwall carbon nanotube (MWCNT) were purchased from Iran's Research Institute of Petroleum Industry (synthesized by chemical vapor deposition (CVD)) with the purity of 95% and the average wall thickness and length were about 40 nm and several micrometers, respectively). 0.01 M phosphate buffered solution (PBS) at pH 7.4 and 6.4 were prepared using distilled water.

Instrumentation

All electrochemical experiments were performed by using three-electrode in a cell containing a working electrode, Ag/AgCl electrode as the reference electrode and a Pt electrode as the counter at room temperature. Also, PalmSens4 potentiostat device (Palm Instrument BV, the Netherlands) with PS-Trace 5 software was used for all measurements including CV, SWV and EIS.

Methods

For all electrochemical measurements, 5 mM $[Fe(CN)_6]^{3-/4-}$ prepared in 0.1 M KCl solution was used as the probe. CV and EIS methods were used to investigate the surface properties at each step of the electrode modification. Also, SWV method was applied for determination of target antigen as well. CV measurements were performed in the potential range of − 0.1 to 0.6 V with scan rate of 0.1 Vs^{-1} and SWV measurements were also performed in the same potential range, with amplitude of 0.025 V at frequency of 25 Hz. The EIS measurements were performed over a frequency range of 1 Hz to 1 MHz at DC potential of 0.2 V with AC amplitude of 0.01 V.

Preparation of the immunosensor

The GCE (2 mm in diameter) was polished with 0.3 and 0.05 µM alumina slurry, respectively. Then, it was washed with distilled water and dried at room temperature to obtain a mirror-like surface. Then, 2 µl of MWCNT solution (0.4 $mgml^{-1}$ in DMF) was casted onto the electrode surface and dried for 1 h at room temperature. At that time, MWCNT/GCE was used for deposition of AuNPs on the electrode surface via placing it in the electrochemical cell containing solution of 10 $mgml^{-1}$ $HAuCl_4$ in 0.1 M KNO_3, and then, potential step of -0.4 V was applied to it, for 10 s. After removing the electrode from the cell, it was washed with distilled water and dried at room temperature. To form SAMs, AuNPs/MWCNT/GC electrode was placed overnight in MUA-MPA solution. The next day, the electrode was rinsed by PBS solution to remove the unbounded molecules, and then, it was immersed in EDC-NHS solution for 1 h, to activate the carboxyl groups, for further binding to the protein amine groups. Then, it was washed again with PBS (pH = 7.4) solution and dried at room temperature.

The antibody immobilization and the antigen detection

Immobilization of the antibody was done through two steps. First, 5 µl of PrG solution (300 μgml^{-1}) in PBS (pH = 7.4) was casted onto AuNPs/MWCNT/GC electrode surface, and then, incubated at 37 °C for 1 h. After washing the electrode, 5 µl of the antibody solution (600μgml^{-1}) in PBS (pH = 6.4) (Akerström and Björck 1986) was added to the electrode surface and incubated overnight, which was, followed by washing with buffer to remove the probable excessive molecules.

Finally, to prevent non-specific bindings and blocking of unreacted sites, the prepared immunosensor was incubated with 5 µl of BSA in PBS (pH = 7.4) solution for 30 min. The electrode was thoroughly washed with PBS (pH = 7.4) and dried before the detection step. To detect the antigen, the prepared immunosensor was incubated for 50 min with standard solutions of NDV in PBS (pH = 7.4) (Armstrong 2008) in the concentration range of 10 to 10^5 $EID_{50}ml^{-1}$. The steps of electrode preparation are schematically illustrated as scheme 1.

Results and discussion

Morphological characterization of the immunosensor

The surface morphology of the modified electrode was investigated using SEM. Figure 1a and b show the SEM images of the GCE after modification with MWCNTs (GCE/MWCNT) and AuNPs (GCE/MWCNT/AuNPs), respectively. As shown in Fig. 1a, MWCNTs have adequately covered the surface. Since, it has been distributed uniformly on the electrode penetrable and homogeneous surface has been reached.

Figure 1b displays the electrodeposited AuNPs on the surface of MWCNTs/GCE. The amount and size of the gold particles, which could be affected by the electrodeposition time, have relatively uniform distribution with approximately size of 50 to 100 nm (with average size of 73 nm).

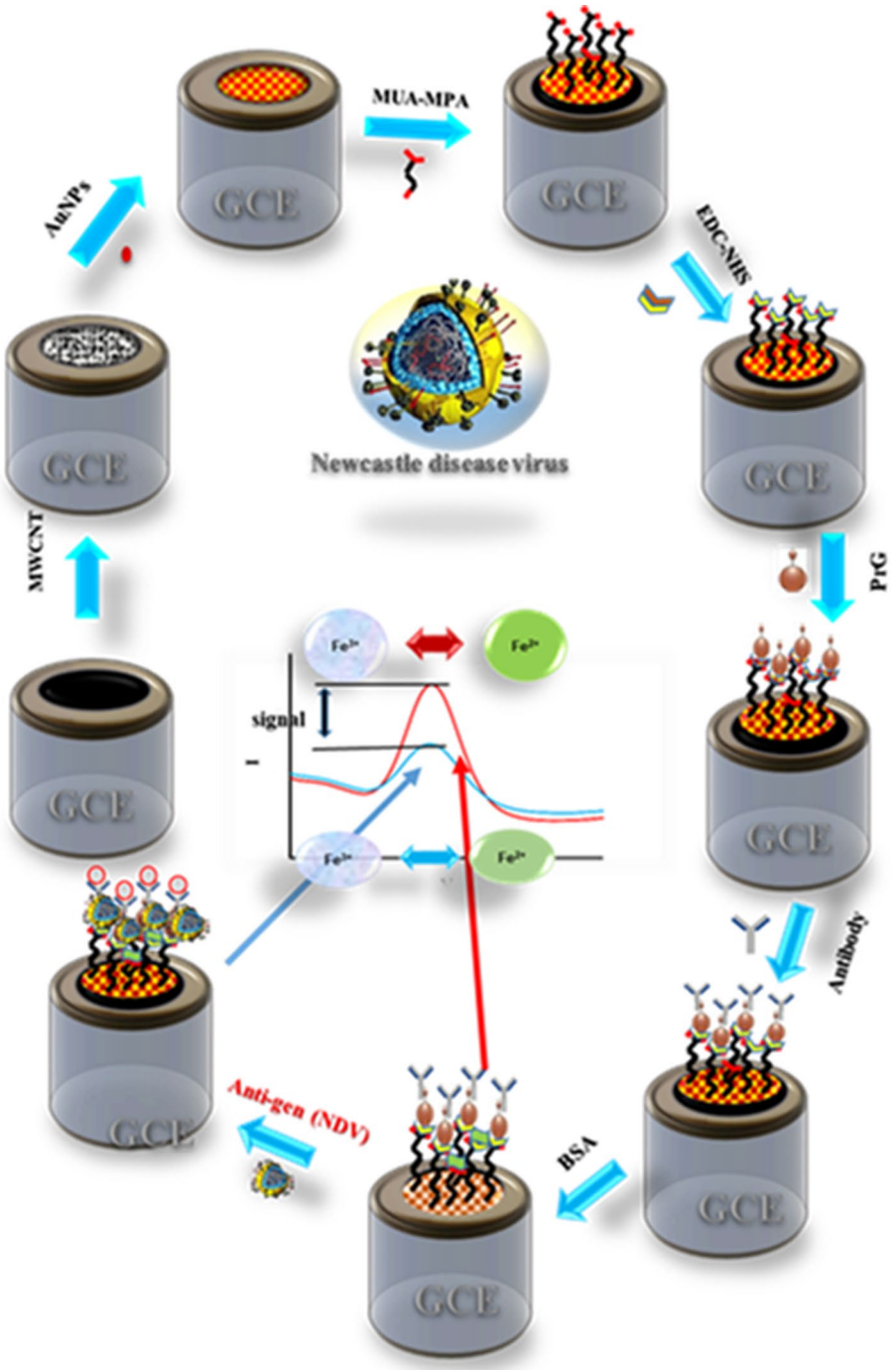

Scheme1 The immunosensor fabrication steps

This could provide a large and efficient surface for adsorption of MUA-MPA and formation SAMs layer on the electrode surface.

For the materials characterization which are used in the electrode modification, FTIR spectra of MWCNTs were recorded as shown in the Fig. 1c. As seen, in the range of 1590–1650 cm^{-1}, in which the stretching vibration mode appeared for the C=O group. Figure 1d demonstrates the UV–vis spectra of MWCNTs (a), which shows a prominent peak at 545 nm attributed to π–π^* transitions of aromatic C=C bonds, and spectra of MWCNTs/AuNPs solution (b), which has two prominent peaks at 530 nm and 260 attributed to the characteristic Plasmon resonance band for AuNPs.

Figure 1e shows the XRD pattern of MWCNT/AuNPs, which contains diffraction a peak at 2θ of 31.5° due to the carbon atoms of MWCNT and four diffraction peaks at the 2θ angles of 38.5°, 44.6°, 64.8° and 77.9°, which were recognized (based on JCPDS, card no. 04–0784) for the

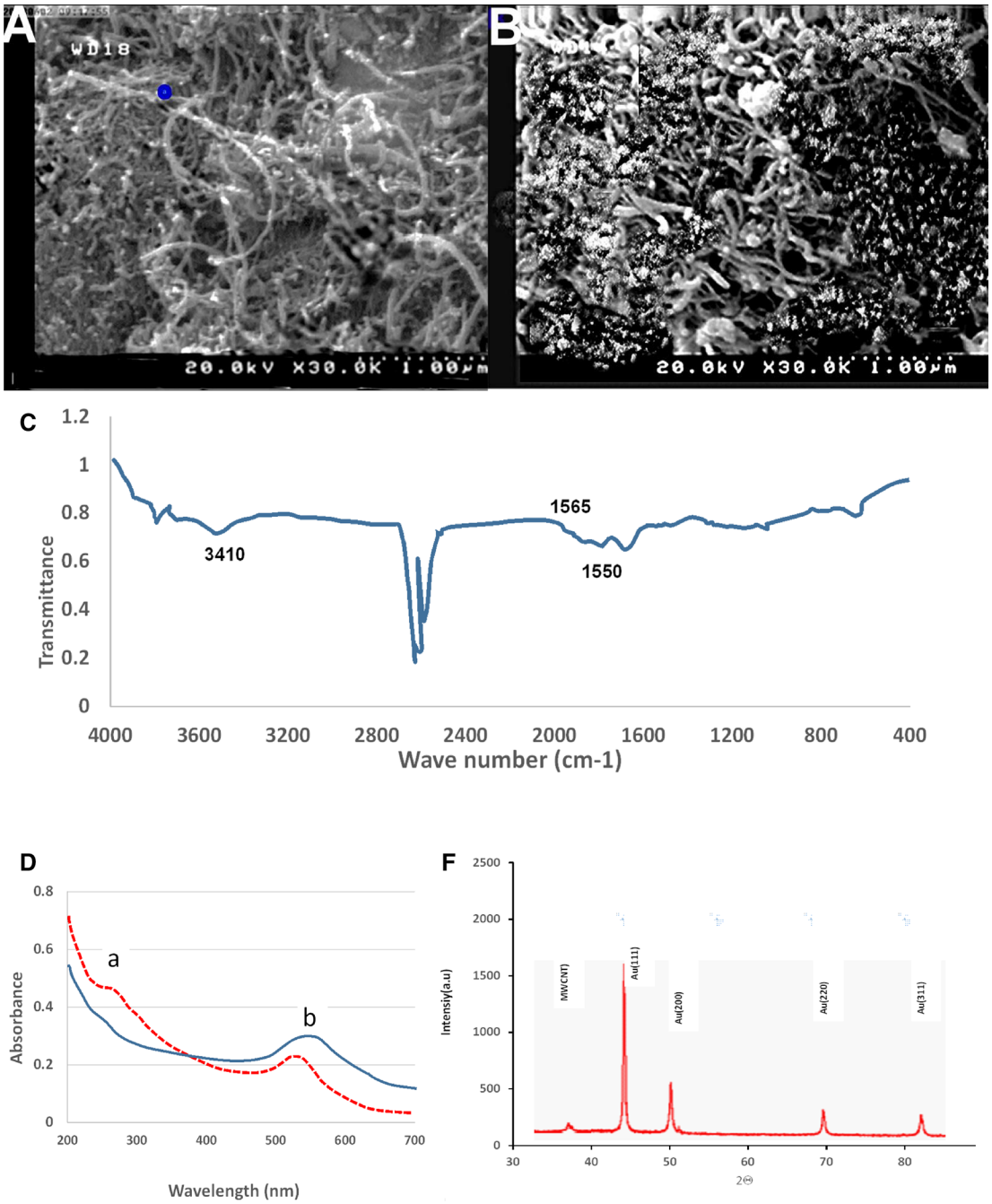

Fig. 1 SEM images of the electrode after modification with **a** MWCNTs and **b** AuNPs/ MWCNTs, **c** FTIR image of MWCNT, **d** UV–Vis absorption spectra of (**a**) MWCNTs and (**b**) AuNPs /MWCNTs solution and **e** XRD pattern of AuNPs loaded on MWCNTs

face-centered cubic structure (111), (200), (220) and (311) of the formed AuNPs, respectively.

Electrochemical characterization of the immunosensor

As stated, CV and EIS techniques were used to evaluate electrode surface characterization at each step of modification. Figures 2 and 3 show CVs and Nyquist curves of the bare GCE, GCE/MWCNT, GCE/MWCNT/AuNPs, GCE/MWCNT/ AuNPs/MUA-MPA, GCE/MWCNT/AuNPs/MUA-MPA/PrG, GCE/MWCNT/AuNPs/MUA-MPA/PrG/Anti-NDV and GCE/MWCNT/AuNPs/MUA-MPA/PrG/Anti-NDV/NDV electrodes in the probe solution (5 mM $[Fe(CN)_6]^{3-/4-}$ and 0.1 M KCl at pH 7.4) at a scan rate of 100 mV. As shown in Fig. 2, after

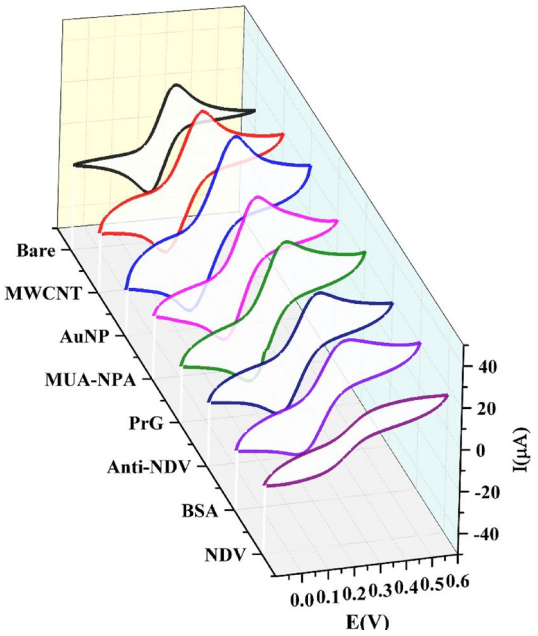

Fig. 2 Cyclic voltammograms of modification steps in PBS solution, pH 7.4, containing 5 mM $[Fe(CN)_6]^{3-/4-}$ prepared in 0.1 M KCl solution and the scan rate of 0.1 Vs^{-1} in the potential range of -0.1 to + 0.6 V

casting of MWCNTs (curve b) and AuNPs (curve c) on the bare GCE (curve a), the redox peak current significantly increased due to the surface enhancement and electrical conductivity of the electrode materials. As expected, the peak current decreased with the consecutive addition of MUA-MPA (curve d), PrG (curve e), antibody (curve f), and BSA (curve g), which is an indication of formation a larger mass transfer barriers toward the probe diffusion at the interface region, which could limit the electron transfer at the electrode surface. Eventually, the redox peak current diminution is a good sign of the successfulness of the fabrication processes. Finally, after NDV trapping, the peak current decreased sharply (curve h), which is due to the fact that the immunocomplex was formed at the electrode surface and made the probe diffusion much more difficult.

To have more conformation about the obtained CV data, EIS could be considered as of complementary and effective technique. Theoretically, the semicircular diameter at low frequencies, in the spectra of EIS implies that the electron transfer resistance (R_{ct}) increases by the formation of a new layer on the electrode surface because of the pathway blockages for the redox probe accessibility toward the surface.

As can be seen in Fig. 3, initially the value of R_{ct} in curve a (related to the bare GCE) was 620 Ω, which reduced to 460 Ω after the modification of the electrode surface with MWCNTs (curve b) and after AuNPs deposition (curve c) reached to 140 Ω. This indicates that the charge transfer greatly reduced after formation of AuNPs/MWCNT/GCE due to existence of the martial with higher conductivity on the surface.

Whereas, as shown in other curves in Fig. 3, after modification of the surface with MUA-MPA (curve d), then with PrG (curve e), antibody (curve f) and BSA (curve

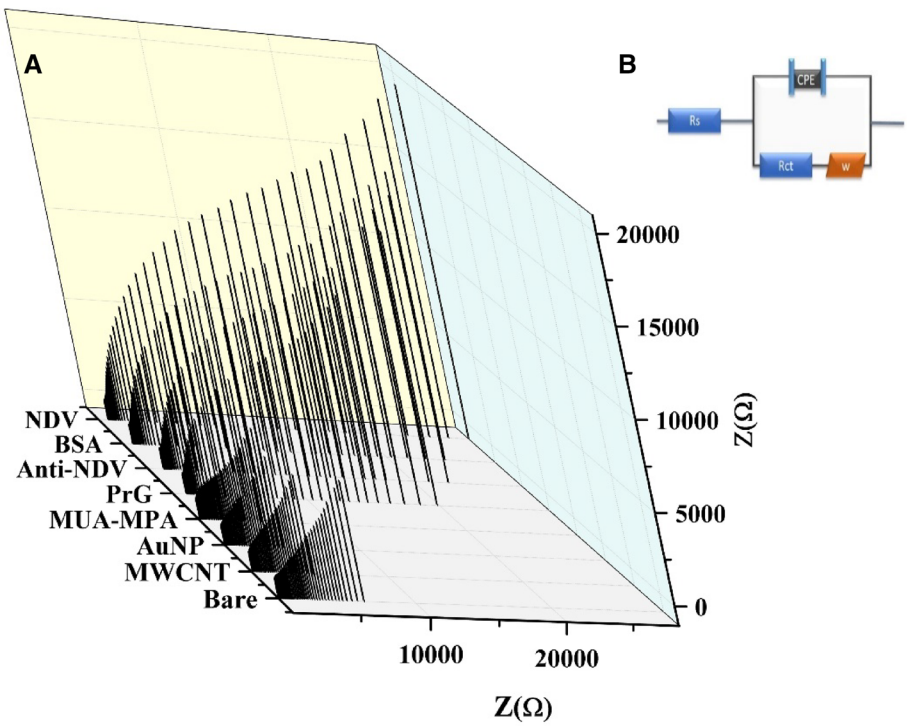

Fig. 3 **a** Nyquist plots of different modification steps in PBS solution, pH 7.4, containing 5 mM $[Fe(CN)_6]^{3-/4-}$ prepared in 0.1 M KCl solution at a DC potential of 0.2 V with AC amplitude of 0.01 V over a frequency range of 1 Hz to 1 MHz and **b** The equivalent circuit for the fabricated immunosensor

g), the diameter of the semicircle increased as well as R_{ct} changes to 1270 Ω, 1625 Ω, 1750 Ω and 1845 Ω, respectively. This confirms the CV data and points to the fact that the electrode impedance (R_{ct}) has grew proportionally with the diffusion limitation for the probe at each step.

Finally, in the incubation of GCE/MWCNT/AuNPs/MUA-MPA/PrG/Anti-NDV with NDV (curve h), the charge transfer (R_{ct}) increased sharply to 2182 Ω, which shows lower diffusion rate of the redox probe and less current due to the formation of immunocomplex at the electrode surface.

This was observed as a decline in the peak current of the voltammograms. Based on the obtained results, the data was in acceptable harmony with the equivalent circuit (Fig. 3b).

Optimization of effective parameters on immunosensor efficiency

From analytical point of view, in order to reach to maximum performance of GCE/MWCNT/AuNP/MUA-MPA/PrG/Anti-NDV/NDV (immunosensor), it is required to optimize the important parameters, such as MWCNT concentration, electrodeposition time of AuNPs, concentration and loading time of PrG, antibody concentration and antigen incubation time.

In the modification of the electrode, the amount of MWCNT and AuNPs are very important parameters, because the surface area and conductivity of the immunosensor is highly dependent to them. To obtain the proper amount of MWCNT in the modified layer, the effect of casted MWCNT concentration in the range of 200 to 800 $\mu g ml^{-1}$ was examined. In this direction, several SW voltammograms of the immunosensor in solution of to 10^3 $EID_{50} ml^{-1}$ NDV and 5 mM $Fe(CN)_6]^{3-/4-}$ and 0.01 M Phosphate buffered solution (PBS) at pH 7.4, were reordered in the potential range of − 0.1 to 0.6 V. As displayed in Fig. 4, the best response for the immunosensors for concentration of 400 $\mu g ml^{-1}$ of MWCNT.

The main reasons for the enhancement of the response before the optimized value could be the electrode surface improvement. However, at higher concentrations than 400 $\mu g ml^{-1}$, the decline in the response could be related to the lower conductivity of the surface. Under the same conditions, the effect of the time of AuNPs electrodeposition on the immunosensor response was studied in the time range of 5 to 30 s. As shown in Fig. 4, the optimum electrodeposition time was 20 s.

The response of GCE/MWCNT/AuNPs/MUA-MPA/PrG/Anti-NDV to 10^3 $EID_{50} ml^{-1}$ NDV was evaluated by varying the concentration of antibody in range of 200 to 1000 $\mu g ml^{-1}$ and PrG concentration in range of 100 to 400 $\mu g ml^{-1}$ in 5 mM $[Fe(CN)_6]^{3-/4-}$ and 0.01 M Phosphate buffered (PBS) at pH 7.4.

As shown in Fig. 5, the highest peak currents were observed for 600 $\mu g ml^{-1}$ of antibody. This indicates that increasing the antibody concentration up to 600 $\mu g ml^{-1}$ on the electrode surface could have enhanced the active sites for the adsorption the NDV species. However, at higher concentrations of the antibody, NDV could not be attached to

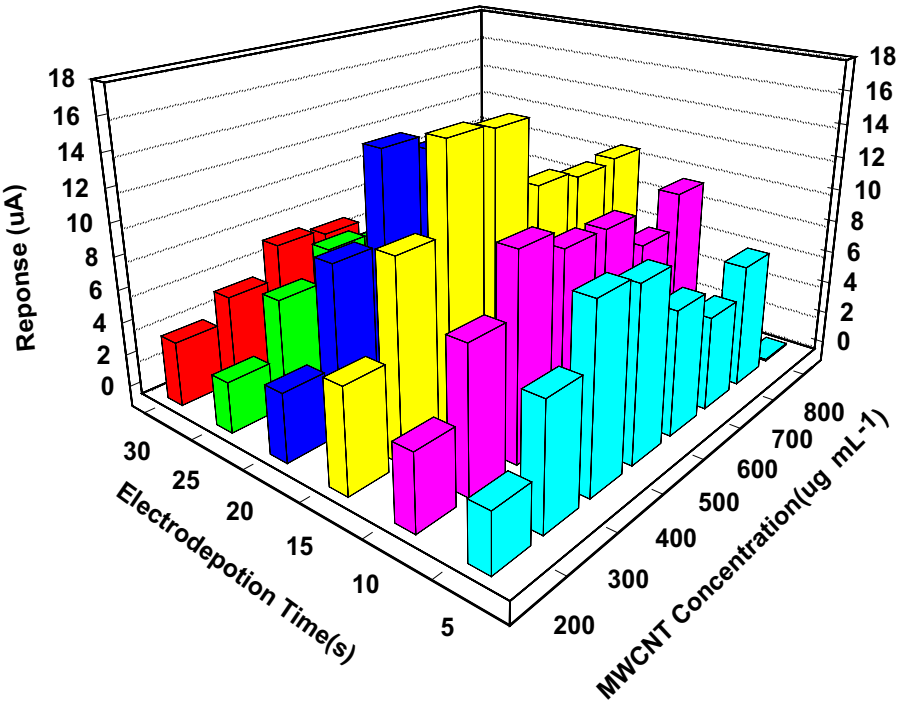

Fig. 4 The SWV response of the immunosensor (incubated with 10^3 $EID_{50} ml^{-1}$ NDV) in 5 mM $[Fe(CN)_6]^{3-/4-}$ and 0.01 M PB at pH 7.4, the potential range of − 0.1 to 0.6 V, for different times of AuNPs electrodeposition and different concentrations of MWCNT solution (range of 200 to 800 $\mu g ml^{-1}$)

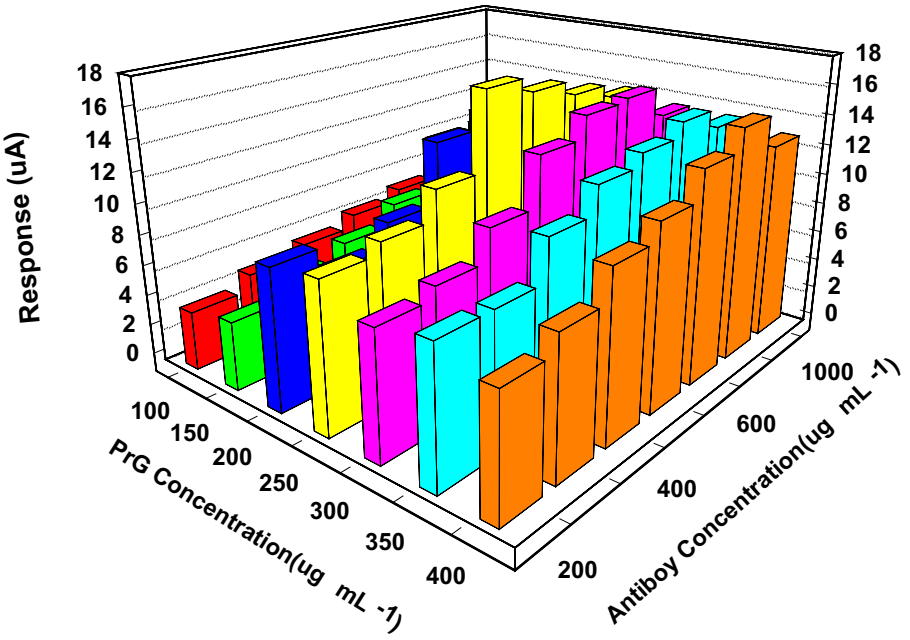

Fig. 5 The SWV response of the immunosensor (incubated with 10^3 $EID_{50}ml^{-1}$ NDV) in 5 mM $[Fe(CN)_6]^{3-/4-}$ and 0.01 M PB at pH 7.4, the potential range of − 0.1 to 0.6 V for the antibody concentration range of (200 to 1000 μgml^{-1}) and PrG concentration in the range of (100 to 400 μgml^{-1})

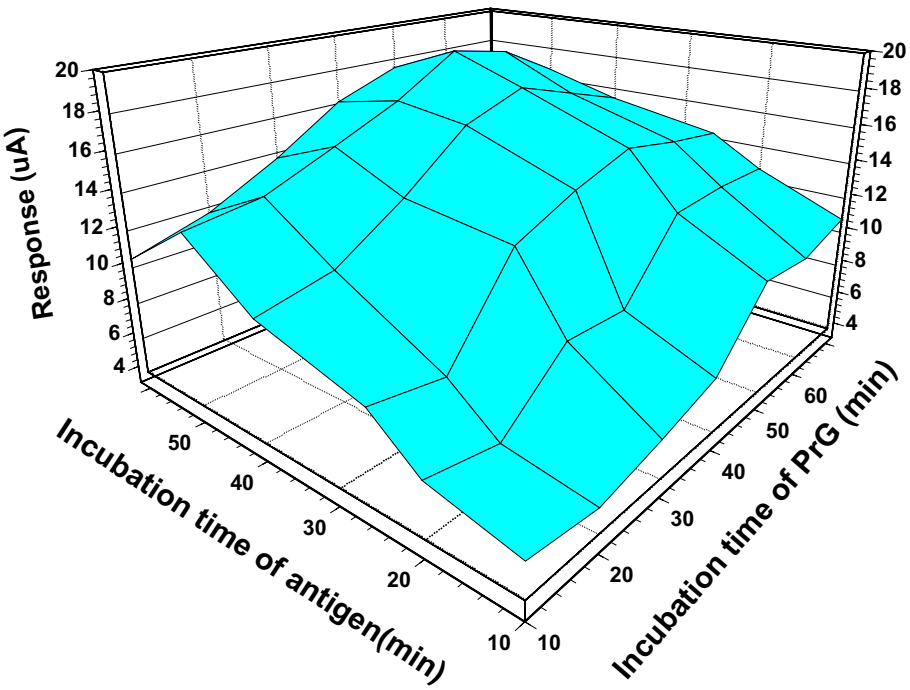

Fig. 6 The SWV response of the immunosensor in 5 mM $[Fe(CN)_6]^{3-/4-}$ and 0.01 M PB at pH 7.4 (after incubated with 10^5 $EID_{50}ml^{-1}$ NDV), the potential range of − 0.1 to 0.6 V, at different PrG incubation time values (10 to 70 min) and antigen loading times (10 to 60 min)

the surface (and/or washed out). For the same reason at concentrations of PrG up to 300 μgml^{-1} the response increased. However, at concentrations higher than 300 μgml^{-1} for PrG, the signal was almost constant. Therefore, 300 μgml^{-1} were selected as the optimum concentration of PrG.

Another important factor in the detection system was the incubation time of PrG and antigen. At this stage, the SWV response of the immunosensor to the 10^3 $EID_{50}ml^{-1}$ NDV was measured after incubation of PrG from 10 to 70 min. The results are shown in Fig. 6, which indicated that up to 50 min, the immunosensor response increased by the time, but at that time the response decreased slightly. This means that the incubation process at 60 min reached to equilibrium, therefore, the time was selected as optimum value.

In order to obtain maximum efficiency, the incubation time of the analyte should be optimized. Therefore, the SWV response of the immunosensor in various antigen incubation time values (10 to 60 min) was evaluated (using

10^3 $EID_{50}ml^{-1}$ NDV,) in 5 mM $[Fe(CN)_6]^{3-/4-}$ and 0.01 M PBS at pH 7.4). As can be seen in Fig. 6, by increasing the interaction time between antigen and GCE/MWCNT/AuNPs/MUA-MPA/PrG/Anti-NDV up to 50 min, the peak current continuously increased. But, at longer times there was no noticeable change in the immunosensor response on account of saturation of the electrode surface. Consequently, the incubation time of 50 min was chosen as the optimal value for the incubation time.

Performance of the immunosensor

Calibration curve

As described in Scheme 1, the formation of the immunocomplex, on the surface of GCE/MWCNT/AuNPs/MUA-MPA/PrG/ Anti-NDV could limit the redox probe access to the surface and cause decline in the peak current. Therefore, in this detection method, the value of current reduction amplified with NDV concentration. The prepared immunosensor was incubated under optimal conditions in the concentration range of 10 to 10^5 $EID_{50}ml^{-1}$. As shown in Fig. 7, the recorded SW voltammograms of the immunosensor after incubated with NDV samples in 5 mM $[Fe(CN)_6]^{3-/4-}$ and 0.01 M PB at pH 7.4 solution) were recorded, and in the potential range from − 0.1 to 0.6 V and amplitude of 0.025 V at a frequency of 25 Hz and antigen incubation time of 50 min.

The immunosensor response ΔI_p, was calculated based on this equation;

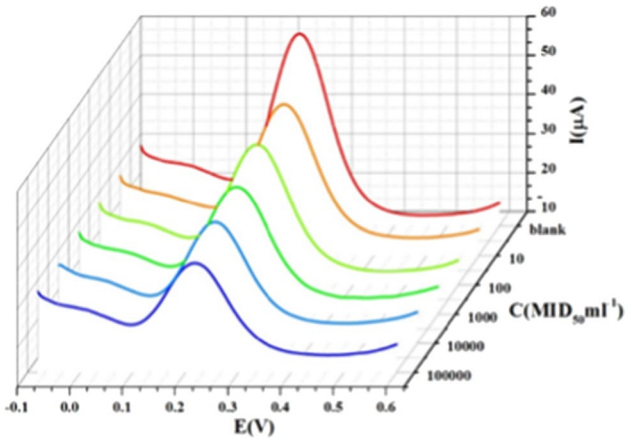

Fig. 7 The SW voltammograms of prepared immunosensor in solutions containing 5 mM $[Fe(CN)_6]^{3-/4-}$ and 0.1 M KCl after incubation with 10, 10^2, 10^3, 10^4 and 10^5 $EID_{50}ml^{-1}$ NDV, amplitude 0.025 V, frequency of 25 Hz in the potential range of − 0.1 to 0.6 V and amplitude of 0.025 V at a frequency of 25 Hz and antigen incubation time of 50 min

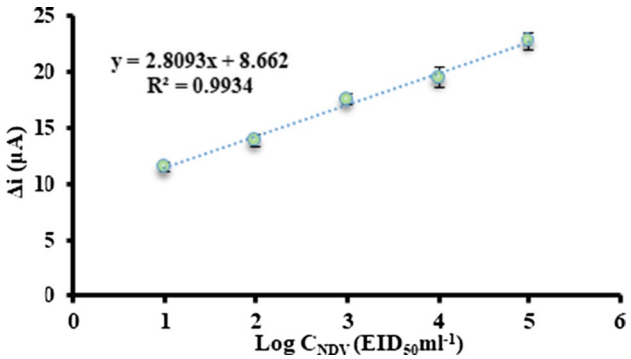

Fig. 8 The immunosensor response against NDV concentration in the range of 10 to 10^5 $EID_{50}ml^{-1}$ in 5 mM $[Fe(CN)_6]^{3-/4-}$ solution prepared in 0.1 M KCl and 0.01 M PB at pH 7.4 (amplitude of 0.025 V, frequency of 25 Hz in the potential range of − 0.1 to 0.6 V)

$$\Delta I_p(\mu A) = I_{po} - I_p \quad (1)$$

where I_{po} is the peak current value in the absence of the analyte and I_p is the peak current for various concentrations of NDV. The calibration curve for the mentioned concentrations vs. ΔI_p, is shown in Fig. 8. (in which for each point three measurements were performed). As seen, there was linear relationship between the electrode response and NDV concentration logarithm with regression of 0.993;

$$\Delta I_p(\mu A) = 2.809\left(\log \text{CNDV}\left(EID_{50}/ml\right)\right) + 8.662 \quad (2)$$

The calculated LOQ was 10 $EID_{50}ml^{-1}$ and the calculated value of the LOD (S/N = 3) was 1.6 $EID_{50}ml^{-1}$. Also, the obtained RSD was less than 4.8%.

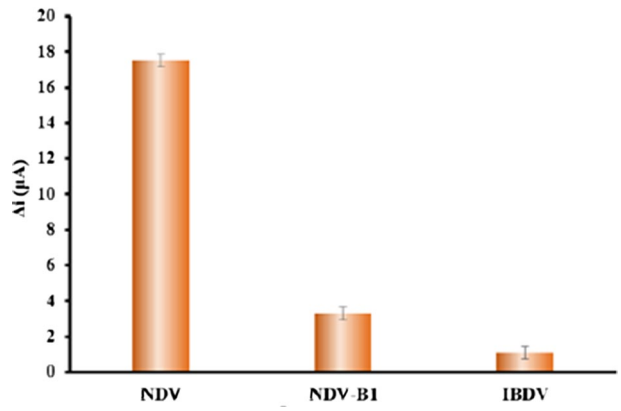

Fig. 9 The SWV response of the immunosensor (incubated with 10^3 $EID_{50}ml^{-1}$ NDV, 10^4 $EID_{50}ml^{-1}$ NDV-B1 and IBDV) in 5 mM $[Fe(CN)_6]^{3-/4-}$ solution prepared in 0.1 M KCl and 0.01 M PB at pH 7.4, the potential range of − 0.1 to 0.6 V

Table1 Immunosensor results in spiked samples

Added (EID_{50}/ml)	Found (EID_{50}/ml)	Recovery (%)	RSD (%)
0	–	–	–
10	9.6	96.0	4.5
10^3	945.0	94.5	3.1
10^5	910,333.3	92.0	1.1

Selectivity

The biosensor selectivity was assessed by measuring its SWV responses to 10^3 $EID_{50}ml^{-1}$ NDV, 10^4 $EID_{50}ml^{-1}$ B1 strains NDV (NDV-B1) and IBDV (Gambro disease virus) under the optimum condition.

Figure 9 illustrates measured SWV response of the immunosensor response at amplitude 0.025 V and frequency of 25 Hz in the potential range of − 0.1 to 0.6 V, in 5 mM $[Fe(CN)_6]^{3-/4-}$ and 0.1 M KCl of the samples. As seen, the immunosensor response to IBDV was very low compared to response of NDV-B1, which indicated a poor interaction between the antibody and IBDV (antigen was related to Gambro disease). However, the largest response belonged to NDV, which confirmed the immunosensor adequate selectivity.

Reproducibility and stability

The immunosensor reproducibility was evaluated by measuring the response (ΔI_p) using 5 similar modified electrodes (incubated with 10^3 $EID_{50}ml^{-1}$ NDV) in the probe (5 mM $[Fe(CN)_6]^{3-/4-}$) and 0.1 M KCl solution. The obtained RSD of the electrodes was 6%.

Under the same experimental condition, the stability of three immunosensors was also assessed over a one-month period of time, in which during the measurements the electrodes were stored in the refrigerator at 4 °C. The measurements were taken every 10 days, and the results showed that after 10, 20 and 30 days, the initial response remained constant with percentages of 95, 92 and 90%, respectively.

Real sample analysis

The analytical measurements of chicken blood samples were performed to evaluate the immunosensor performance in real samples. On this purpose, 10, 10^3 and 10^5 $EID_{50}ml^{-1}$ of standard antigen solutions was added to poultry serum (50 times diluted) and was incubated on the surface of the immunosensor, respectively. Then, they were immersed in the probe solution and their SW voltammograms were recorded. The results are presented in Table 1. As it is shown, the relative recoveries corresponding to the actual values had acceptable standard deviations. The small difference in the founded and actual values could be due to the matrix influence. These results confirmed that the proposed immunosensor had sufficient accuracy and precision in the real samples analysis.

Conclusion

Herein, a novel sensitive method for early detection of Newcastle disease by stepwise modification of a label free electrochemical immunosensor was introduced. In this method, the antibodies were immobilized on the surface in an orientated manner, so that they could be more effectively stabilized on the surface and exposed to the analyte. To achieve this purpose, PrG fixed on alkane thiols SAMs were used. The parameters affecting the analyte measurement were optimized and the immunosensor showed linear range of response toward the concentration from10 to 10^5 $EID_{50}ml^{-1}$ with LOD of 1.6 $EID_{50}ml^{-1}$ under optimal conditions. Also, the immunosensor had adequate performance to detect NDV in the biological real samples. This method was simple, low cost, quick and unlike other reported methods did not require the probe labeling process, thus it could be effectively used for detecting and controlling the diseases in portable devices.

Acknowledgements The authors would like to appreciate the Research Council of University of Tehran for the financial support of this work.

References

Afkhami A, Hashemi P, Bagheri H, Salimian J, Ahmadi A, Madrakian T (2017) Impedimetric immunosensor for the label-free and direct detection of botulinum neurotoxin serotype A using Au nanoparticles/graphene-chitosan composite. Biosensors Bioelectron 93:124–131

Akerström B, Björck L (1986) A physicochemical study of protein G, a molecule with unique immunoglobulin G-binding properties. J Biol Chem 261:10240–10247

Alves RC, Pimentel FB, Nouws HP, Silva TH, Oliveira MBP, Delerue-Matos C (2017) Improving the extraction of Ara h 6 (a peanut allergen) from a chocolate-based matrix for immunosensing detection: Influence of time, temperature and additives. Food Chem 218:242–248

Armstrong B (2008) Antigen–antibody reactions. ISBT Sci Ser 3:21–32

Baniukevic J, Boyaci IH, Bozkurt AG, Tamer U, Ramanavicius A, Ramanaviciene A (2013) Magnetic gold nanoparticles in SERS-based sandwich immunoassay for antigen detection by well oriented antibodies. Biosens Bioelectron 43:281–288

Berto M et al (2019) Label free detection of plant viruses with organic transistor biosensors. Sensors Actuat B Chem 281:150–156

Chaka H, Thompson PN, Goutard F, Grosbois V (2015) Evaluation of enzyme-linked immunosorbent assays and a haemagglutination inhibition tests for the detection of antibodies to Newcastle disease

virus in village chickens using a Bayesian approach. Prevent Veterinary Med 119:21–30
Chen H-t, Zhang J, Sun D-h, Ma L-n, Liu X-t, Cai X-p, Liu Y-s (2008) Development of reverse transcription loop-mediated isothermal amplification for rapid detection of H9 avian influenza virus. J Virol Methods 151:200–203
Chen J et al (2018) Development and application of a SYBR green real-time PCR for detection of the emerging avian leukosis virus subgroup K. Poult Sci 97:2568–2574
Cong F, Zhu Y, Liu X, Li X, Chen M, Huang R, Guo P (2018) Development of an xTAG-multiplex PCR array for the detection of four avian respiratory viruses. Mol Cell Probes 37:1–5
De Wit J, Davelaar F, Braunius W (1992) Comparison of the enzyme linked immunosorbent assay, the haemagglutination inhibition test and the agar gel precipitation test for the detection of antibodies against infectious bronchitis and Newcastle disease in commercial broilers. Avian Pathol 21:651–658
Dhar PK, Dutta A, Das A, Jalal MS, Barua H, Biswas PK (2018) Validation of real-time reverse transcription polymerase chain reaction to detect virus titer and thermostability of Newcastle disease live virus vaccine Veterinary. World 11:1597
Ebrahimi M, Norouzi P, Safarnejad MR, Tabaei O, Haji-Hashemi H (2019) Fabrication of a label-free electrochemical immunosensor for direct detection of Candidatus Phytoplasma Aurantifolia. J Electroanal Chem 851:113451
Eissa S et al (2018) Carbon nanofiber-based multiplexed immunosensor for the detection of survival motor neuron 1, cystic fibrosis transmembrane conductance regulator and duchenne muscular dystrophy proteins. Biosensors Bioelectron 117:84–90
Eissa S, Alshehri N, Rahman AMA, Dasouki M, Abu-Salah KM, Zourob M (2018) Electrochemical immunosensors for the detection of survival motor neuron (SMN) protein using different carbon nanomaterials-modified electrodes. Biosensors Bioelectron 101:282–289
Fan Z, Keum YS, Li QX, Shelver WL, Guo L-H (2012) Sensitive immunoassay detection of multiple environmental chemicals on protein microarrays using DNA/dye conjugate as a fluorescent label. J Environ Monit 14:1345–1352
Fellahi S et al (2016) Comparison of SYBR green I real-time RT-PCR with conventional agarose gel-based RT-PCR for the diagnosis of infectious bronchitis virus infection in chickens in Morocco. BMC Res Notes 9:231
Garnier R et al (2017) Interpreting ELISA analyses from wild animal samples: Some recurrent issues and solutions. Funct Ecol 31:2255–2262
Ghanavati M, Tadayon F, Bagheri H (2020) A novel label-free impedimetric immunosensor for sensitive detection of prostate specific antigen using Au nanoparticles/MWCNTs-graphene quantum dots nanocomposite. Microchem J 159:105301
González-MartÍnez MA, Penalva J, Puchades R, Maquieira A, Ballesteros B, Marco MP, Barceló D (1998) An immunosensor for the automatic determination of the antifouling agent Irgarol 1051 in natural waters. Environ Sci Technol 32:3442–3447
Haji-Hashemi H, Norouzi P, Safarnejad MR, Ganjali MR (2017) Label-free electrochemical immunosensor for direct detection of Citrus tristeza virus using modified gold electrode. Sensors Actuat B Chem 244:211–216
Haji-Hashemi H, Norouzi P, Safarnejad MR, Larijani B, Habibi MM, Raeisi H, Ganjali MR (2018) Sensitive electrochemical immunosensor for citrus bacterial canker disease detection using fast Fourier transformation square-wave voltammetry method. J Electroanal Chem 820:111–117
Haji-Hashemi H, Safarnejad MR, Norouzi P, Ebrahimi M, Shahmirzaie M, Ganjali MR (2019) Simple and effective label free electrochemical immunosensor for Fig mosaic virus detection. Anal Biochem 566:102–106
Hosu O, Tertiș M, Melinte G, Feier B, Săndulescu R, Cristea C (2017) Mucin 4 detection with a label-free electrochemical immunosensor. Electrochem Commun 80:39–43
Huang J et al (2020) Electrochemical immunosensor with Cu (I)/Cu (II)-chitosan-graphene nanocomposite-based signal amplification for the detection of newcastle disease virus. Sci Rep 10:1–12
Kausaite-Minkstimiene A, Ramanaviciene A, Kirlyte J, Ramanavicius A (2010) Comparative study of random and oriented antibody immobilization techniques on the binding capacity of immunosensor. Anal Chem 82:6401–6408
Kothlow S, Häuslaigner R, Kaspers B, Grund C (2008) Evaluation of Newcastle disease virus immunoassays for waterfowl using a monoclonal antibody specific for the duck immunoglobulin light chain. Avian Pathol 37:323–328
Laamiri N, Aouini R, Marnissi B, Ghram A, Hmila I (2018) A multiplex real-time RT-PCR for simultaneous detection of four most common avian respiratory viruses. Virology 515:29–37
Li Q et al (2019) Evaluation of an immunochromatographic strip for detection of avian avulavirus 1 (Newcastle disease virus). J Veterinary Diagnostic Investigat 31:475–480
Lin D, Pillai RG, Lee WE, Jemere AB (2019) An impedimetric biosensor for *E. coli* O157: H7 based on the use of self-assembled gold nanoparticles and protein G. Microchim Acta 186:1–9
Mackiewicz M, Marcisz K, Strawski M, Romanski J, Stojek Z, Karbarz M (2018) Modification of gold electrode with a monolayer of self-assembled microgels. Electrochim Acta 268:531–538
Makaraviciute A, Ruzgas T, Ramanavicius A, Ramanaviciene A (2014) Antibody fragment immobilization on planar gold and gold nanoparticle modified quartz crystal microbalance with dissipation sensor surfaces for immunosensor applications. Anal Methods 6:2134–2140
Martínez Rojas FJ (2020) Desarrollo de un inmunosensor electroquímico para la detección de biomarcador específico de cáncer
Mirzaei S, Shoushtari A, Nouri A (2018) Development and evaluation of real-time RT-PCR test for quantitative and qualitative recognition of current H9N2 subtype avian influenza viruses in Iran. Arch Razi Inst 73:177–182
Mirzaei S, Shoushtari A, Nouri A (2020) Development and evaluation of real-time reverse transcription polymerase chain reaction test for quantitative and qualitative recognition of H5 subtype of avian influenza viruses. Arch Razi Inst 75:17–22
Mollarasouli F, Serafín V, Campuzano S, Yáñez-Sedeño P, Pingarrón JM, Asadpour-Zeynali K (2018) Ultrasensitive determination of receptor tyrosine kinase with a label-free electrochemical immunosensor using graphene quantum dots-modified screen-printed electrodes. Anal Chim Acta 1011:28–34
Paiva TO, Almeida I, Marquês JT, Liu W, Niu Y, Jin G, Viana AS (2017) Nanostructured interfaces with site-specific bioreceptors for immunosensing. Appl Surf Sci 412:455–463
Sutton DA et al (2019) Development of an avian avulavirus 1 (AAvV-1) L-gene real-time RT-PCR assay using minor groove binding probes for application as a routine diagnostic tool. J Virol Methods 265:9–14
Taghdisi SM, Danesh NM, Ramezani M, Abnous K (2018) A new amplified fluorescent aptasensor based on hairpin structure of G-quadruplex oligonucleotide-Aptamer chimera and silica nanoparticles for sensitive detection of aflatoxin B1 in the grape juice. Food Chem 268:342–346
Tang S et al (2018) A novel cytosensor based on Pt@ Ag nanoflowers and AuNPs/Acetylene black for ultrasensitive and highly specific detection of circulating tumor cells. Biosensors Bioelectron 104:72–78
Thinh TQ, Quan TVV, Thuy TH, Xuan CT, Tuan MA A label-free electrochemical immunosensor for detection of Newcastle disease virus. In: International Conference on the Development

of Biomedical Engineering in Vietnam, 2018. Springer, pp 699–703

Thirumurugan G, Jayakumar R, Kumanan K, Venugopalan A, Nachimuthu K (1997) Latex immunoassay for rapid detection of Newcastle disease virus Tropical animal health and production. Tropical Animal Health Product 29:227–230

Wang H et al (2019) Establishment of xMAP for the simultaneous detection of antibodies to Newcastle disease virus and avian influenza virus. Poult Sci 98:1494–1499

Wang J, Wang J, Chen P, Liu L, Yuan W (2017) Development of a TaqMan-based real-time PCR assay for rapid and specific detection of fowl aviadenovirus serotype 4. Avian Pathol 46:338–343

Wang R, Feng J-J, Xue Y, Wu L, Wang A-J (2018) A label-free electrochemical immunosensor based on AgPt nanorings supported on reduced graphene oxide for ultrasensitive analysis of tumor marker. Sensors Actuat B Chem 254:1174–1181

Wei S, Xiao H, Cao L, Chen Z (2020) A label-free immunosensor based on graphene oxide/Fe3O4/prussian blue nanocomposites for the electrochemical determination of HBsAg. Biosensors 10:24

Xiao H, Wei S, Chen Z, Cao L (2020) Label-free electrochemical immunosensor based on gold and iron-oxide nanoparticle co-modified rGO-TEPA hybrid for sensitive detection of carcinoembryonic antigen. Electrocatalysis 11(5):513–521

Yao M, Zhang X, Gao Y, Song S, Xu D, Yan L (2019) Development and application of multiplex PCR method for simultaneous detection of seven viruses in ducks. BMC Veterinary Res 15:103

Zhang W et al (2017) Establishment of a high sensitive indirect ELISA for detecting specific antibodies against H9 subtype avian influenza virus Sheng wu Gong Cheng xue bao= Chinese. J Biotechnol 33:1253–1264

Zhang X, Yao M, Tang Z, Xu D, Luo Y, Gao Y, Yan L (2020) Development and application of a triplex real-time PCR assay for simultaneous detection of avian influenza virus, Newcastle disease virus, and duck Tembusu virus. BMC Veterinary Res 16(1):1–12

Zhang Z et al (2019) Multiplex one-step real-time PCR assay for rapid simultaneous detection of velogenic and mesogenic Newcastle disease virus and H5-subtype avian influenza virus. Archives Virol 164:1111–1119